Simple, universal rules predict trophic interaction strengths

Kyle E. Coblentz[1], Mark Novak[2], John P. DeLong[1]

1. School of Biological Sciences, University of Nebraska-Lincoln, Lincoln, NE, USA
2. Department of Integrative Biology, Oregon State University, Corvallis, OR, USA

Many critical drivers of ecological systems exhibit regular scaling relationships[1–3], yet, often, the underlying mechanisms explaining these relationships are unknown. Trophic interactions strengths, which underpin ecosystem stability and dynamics[4–7], are no exception, exhibiting statistical and scaling relationships with predator and prey traits that lack a causal evolutionary explanation[8–11]. Here we propose two universal rules that explain the scaling of trophic interaction strengths through predator functional responses – the relationship between predator feeding rates and prey densities. First, functional responses must allow predators to meet their energetic demands when prey are rare. Second, functional responses should approach their maxima near the highest prey densities that predators experience. We show that parameterized mathematical equations derived from these two rules predict functional response parameters across over 2,100 functional response experiments. They also provide additional predictions including consistent patterns of feeding rate saturation with prey densities among predators, a slow-fast continuum in functional response parameters, and the allometric scaling of those parameters. The two rules thereby offer an ultimate explanation for the determinants of trophic interaction strengths and their scaling, revealing the importance of ecologically realized constraints to the complex, adaptive nature of functional response evolution.

Understanding the ecological and evolutionary determinants of the strengths of predator-prey interactions is key to understanding the stability, diversity, and dynamics of ecosystems[4–7]. A fundamental component of trophic interaction strengths is the predator's so-called functional response that describes how predator feeding rates change with prey density[12,13]. Thousands of experiments have measured functional responses for taxa ranging from microbes to large carnivores in nearly every biome on earth[14] to uncover a wide variety of variables that influence the underlying parameters, including statistical relationships with predator and prey traits[8,10,15–17]. Principal among these are predator and prey body sizes whose consistent allometric relationships with functional response parameters serve as the basis for most dynamical food web models[11,18,19]. However, despite the existence and utility of such statistical relationships between functional response parameters and many traits, it remains unclear *why* these relationships exist as they do.

Early theory suggested that because organisms' metabolic rates scale to approximately the ¾ power with their body masses, that the biomass consumption rates of predators should also scale to the ¾ power[11]. More recent theory considering proximate mechanisms for the strengths of trophic interactions such as the dimensionality of predator-prey interactions and the allometric scaling of predator and prey velocities has seen success in predicting certain functional response parameters (i.e. the space clearance/attack/search rate at low prey density) and their scaling

relationships as well[16,20]. But other parameters (i.e. the asymptotic/maximum feeding rate at high prey density or its reciprocal, the handling time) remain poorly predicted, such that an understanding of the evolutionary drivers of functional responses remains missing. An encompassing means to predict predator foraging rates through a theory that reflects the ultimate causes determining them is therefore still lacking.

Two Rules for Functional Responses

We posit that the functional response of a predator must meet two conditions. First, a predator's feeding rate must meet its energetic demands at the low prey densities it is likely to experience. This must be true for a predator to persist. Second, the prey densities at which a predator's feeding rate saturates should be near the highest prey densities that it is likely to experience. This is because, first, feeding rates must saturate at some prey density[12,21]. Second, if feeding rates saturated at a lower prey density, predators would pay an opportunity cost for missing out on higher feeding rates at the high prey densities they experience. Last, lower handling times (i.e. higher maximum feeding rates) leading to higher feeding rates at high prey densities: i) have diminishing fitness returns since the highest prey densities are rarely experienced, ii) imply less energy extracted per prey consumed[22], and iii) require larger ingestive or digestive capacities that are energetically costly to maintain[23–25]. Past studies on functional response evolution have largely focused on relatively simple optimization of predator feeding rates[26–28]. The two rules we posit take a different view in which functional responses are the outcome of long-term evolution of the traits determining predator functional responses that balance selective pressures on predator traits. The outcome of this evolutionary process is that predators are minimally capable of persisting when prey are scarce while also being able to take advantage of occasionally abundant prey.

We derive two equations encapsulating these two constraints. The first rule that predators must satisfy their metabolic demand at low prey densities can be formalized as

$$D = f_{low} E M_N, \qquad \text{Eqn. 1}$$

where D is the daily energetic demand of the predator determined by its metabolic rate in kJ/day. The rate at which prey are consumed when rare is given by its feeding rate f_{low} which should be well approximated by a linear functional response ($f_{low} = aN_{low}$, where a is the space clearance rate and N_{low} the low prey density)[8,29]. E is the energy density of the prey in units of kJ/g, and M_N is the mass of the prey in grams to convert the number of prey eaten to the mass of prey eaten.

The second rule that a predator's feeding rate should saturate near the highest prey densities it experiences can be formalized as

$$I_S = f_{high} h, \qquad \text{Eqn. 2}$$

where I_S is the degree of saturation ranging between 0 and 1 and h is the handling time (i.e. the inverse of the maximum feeding rate)[8]. Assuming a Holling Type II functional response, as we do here, $f_{high} = \frac{aN_{high}}{1+ahN_{high}}$ where N_{high} is a high density of prey likely to be experienced by the predator. I_S may also be interpreted as the fraction of time that a predator individual is busy

handling prey, or as the fraction of individuals in a predator population that are handling prey at any given point in time (Supplementary Information)[30,31].

Given these two equations, we can solve for the space clearance rate and handling time as

$$a = \frac{D}{N_{low} E M_N} \qquad \text{Eqn. 3}$$

and

$$h = \frac{I_S N_{low} E M_N}{D N_{high} (1 - I_S)}. \qquad \text{Eqn. 4}$$

All parameters on the right-hand side of these equations excepting I_S may be estimated from well-established relationships between organismal mass and metabolic rates (i.e. Kleiber's Law) [2,32] and abundances (i.e. Damuth's Law)[33] or are well approximated as an empirical constant (i.e. an energy density of prey 5.6kJ/g wet weight of prey)[34]. We assume $I_S = 0.9$, but our inferences are robust to choices of this value (Supplementary Information).

Prediction of a and h

The two rules perform well in predicting empirically estimated space clearance rate and handling time values across their respective 19 and 8 orders of magnitude in variation (Figure 1; log space clearance rate correlation coefficient = 0.82, R^2 of 1:1 line = 0.81; log handling time correlation coefficient = 0.57, R^2 of 1:1 line = 0.75). The slopes of major axis regressions between observed and predicted space clearance rates (β = 0.85, 95% Confidence Interval (CI) = 0.82, 0.87) and handling times (β = 1.14, 95% CI = 1.08, 1.22) suggest a tendency for the slight overestimation of space clearance rates and underestimation of handling times at low values, and the underestimation of space clearance rates and overestimation of handling times at high values (Figure 1). Alternative means for determining low and high prey densities and levels of predator saturation shift the points in Figure 1, but do not influence the predictive power of the two rules for empirically reasonable values (Supplementary Information). Indeed, the tendency for over/under-estimation likely reflects insightful across-system variation that is not reflected in estimates from mass-scaling relationships.

To illustrate this, we also predicted the functional response parameters for the subset of the studies that were field studies assuming the minimum and maximum observed prey densities reflect N_{low} and N_{high}. For seven studies of mammalian predators and their prey, we also used system-specific information on energetic demand and the energy density of prey to predict space clearance rates and handling times (Methods). Across all field studies, we again find that the predictions fall near the 1:1 line but without the same systematic tendency for over/under-estimation. Therefore, we conclude that predictions with system-specific information on prey densities, energy densities, and masses are likely to outperform those from empirical scaling rules.

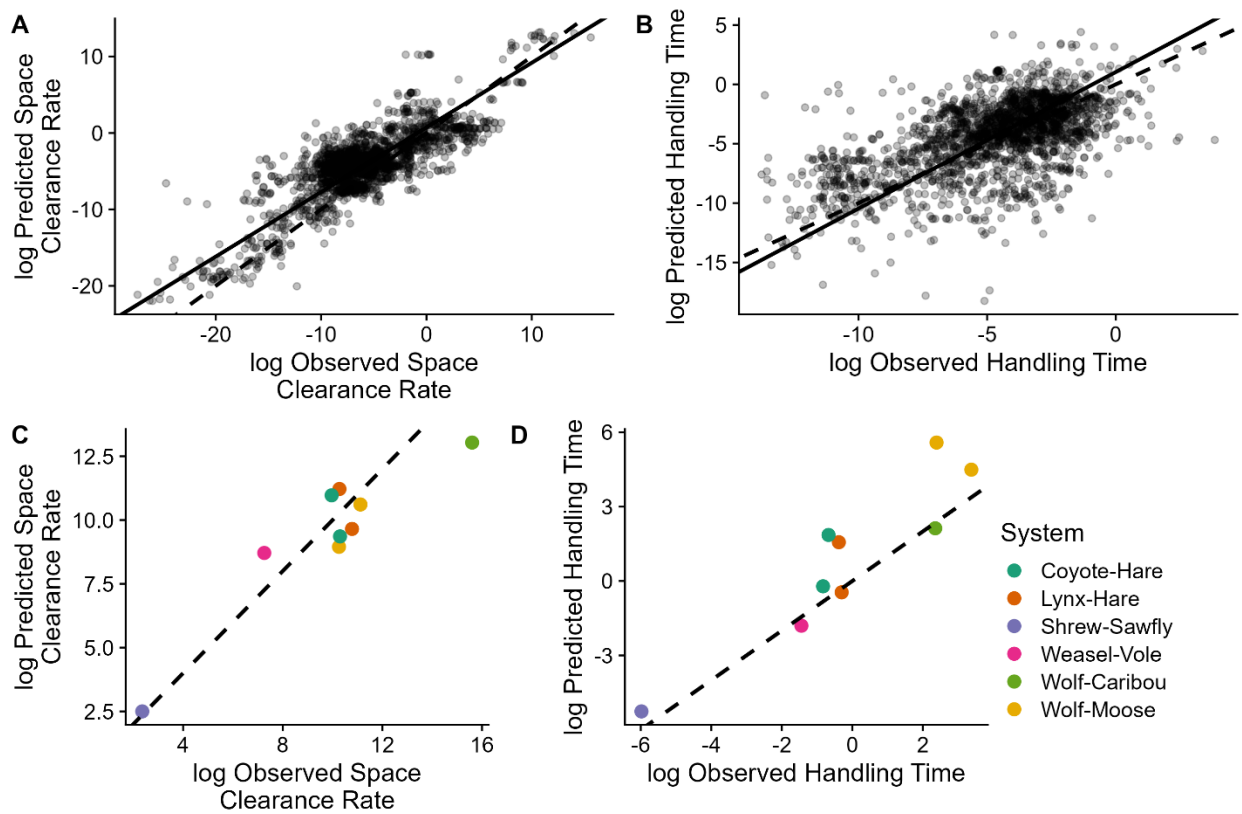

Figure 1. Two simple rules derived from predator feeding rates at low and high prey densities predict space clearance rates and handling times using either generic estimates from empirical mass scaling relationships (A,B) or system-specific estimates from field studies (C,D). Dashed lines are 1:1 lines and solid lines are major axis regressions.

Auxiliary Predictions

The posited rules also predict three auxiliary sets of relationships: a consistent feeding rate saturation pattern among predators, a slow-fast continuum in functional responses, and the allometric scaling of functional response parameters.

First, our second rule implies that space clearance rates and handling times should be related to the high densities of prey that predators experience. Specifically, the so-called half-saturation constant $\frac{1}{ah}$ (the density of prey at which the feeding rate is half its maximum) is predicted to be related to high prey densities as

$$\frac{1}{ah} = \frac{(1-I_S)N_{high}}{I_S}. \qquad \text{Eqn. 5}$$

Plotting the right-hand side of equation 5 against the empirical half-saturation constant values supports this prediction (correlation = 0.86, slope of major axis regression (95% Confidence Interval) = 0.88 (0.86,0.9), Fig. 2A). Since the rules predict that predators should reach saturation

near the high prey densities they are likely to experience, this suggests that patterns of predator feeding rate saturation are likely to be consistent across the range of prey densities experienced by predators. For example, with $I_S = 0.9$, each predator species should reach half their maximum feeding rate at approximately $0.11N_{high}$ despite these species experiencing very different values of N_{high}. This prediction is consistent with previous findings that predator feeding rates are typically unsaturated[8] because the predicted prey density at which half-saturation occurs is typically 2.4 times higher (standard deviation = 0.4) than the predicted median prey density due to the right-skewed nature of population abundances in space and time[35,36].

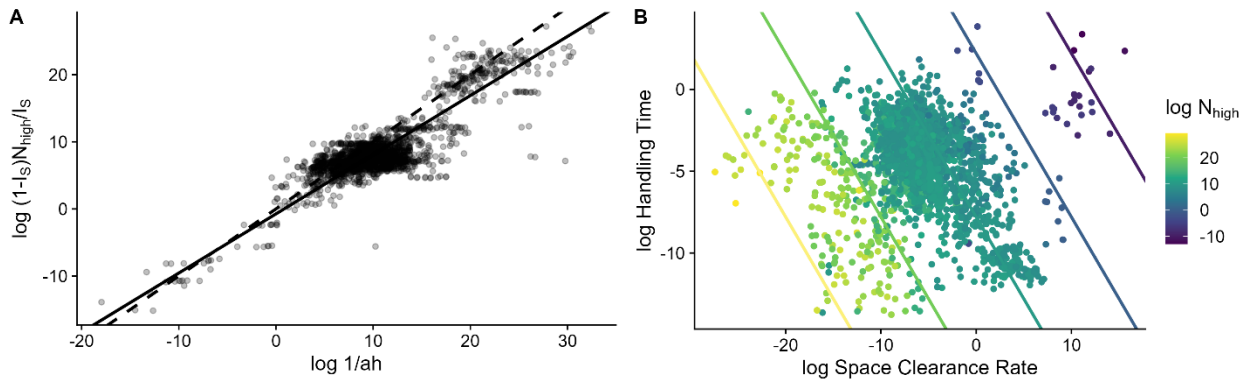

Figure 2. The two rules predict empirical estimates of the half-saturation constant (*1/ah*) (A), as well as the relationship between space clearance rates and handling times (B) using only knowledge of the saturation experienced at high experienced prey densities. The dashed line in A is a 1:1 line and the solid line is a major axis regression. The lines in B are the predicted relationships between space clearance rates and handling times for different values of N_{high}.

Second, the two rules correctly predict that space clearance rates and handling times should be inversely related to each other --- as modified by I_s and N_{high} --- such that

$$ln(h) = ln\left(\frac{I_S}{(1-I_S)N_{high}}\right) - ln(a) \qquad \text{Eqn. 6}$$

(Figure 2B). This relationships contrasts with long-standing theory on species coexistence mechanisms which requires there to be a positive relationship between space clearance rates and handling times for the coexistence of consumers on common resources that are spatially and temporally variable, representing a gleaner-exploiter tradeoff [37,38]. Our predictions are instead consistent with there being a slow-fast continuum whereby predators with high foraging intensity also minimize the time costs of consumption[39], driven evolutionarily by variation in predator energetic demand and prey energy density.

Third, the two rules predict how space clearance rates and handling times scale with predator and prey body masses. Specifically, the empirical scaling of the parameters we consider as being related to body size (those besides I_S and E) are $N_{low} \propto M_N^{-0.94}$, $N_{high} \propto M_N^{-0.9}$, and $D \propto M_P^{0.87}$ where M_P is the mass of the predator and the other parameters are defined above (Methods). Given these scaling relationships and the first rule, it follows that the allometric relationship for the space clearance rate should be $a \propto M_P^{0.87} M_N^{-0.06}$. Given that in the dataset

$M_N \propto M_P^{0.79}$, we therefore predict that $a \propto M_P^{0.82}$. This prediction matches the observed scaling of $a \propto M_P^{0.8}$ (95% confidence interval (CI) = 0.78, 0.83; Figure 3A). Similarly, the allometric relationship for handling time should be $h \propto \mathrm{M_N^{0.96}} M_P^{-0.87}$. Thus, we predict $\frac{h}{M_N} \propto M_P^{-0.87}$. This prediction also matches the observed scaling of $\frac{h}{M_N} \propto M_P^{-0.85}$ (95% CI = -0.87, -0.82; Figure 3B; See Supplemental Information for derivations of scaling relationships).

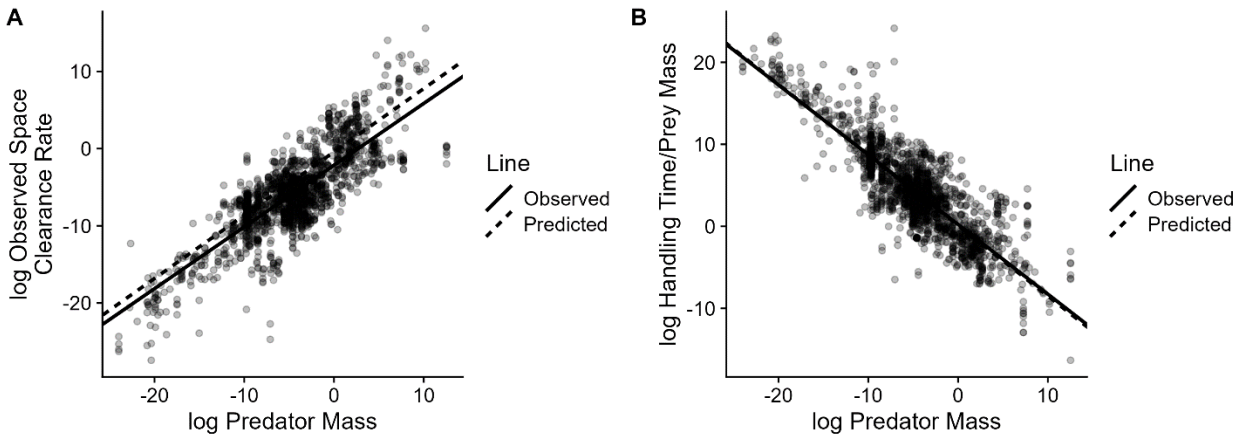

Figure 3. Functional response rules and empirical scaling relationships between parameters and prey and predator masses predict that the log space clearance rate increases with log predator mass with a slope of 0.82 (observed empirical estimate: 0.8, A) and that the log of the prey mass-specific handling time (handling time/prey mass) decreases with log consumer mass with a slope of -0.87 (observed empirical estimate: -0.86; B).

Conclusions

Two simple rules can predict the parameters of predator functional responses and their scaling relationships that govern their impacts on the dynamics and stability of ecosystems. In contrast to prior theory, these rules for predator functional responses provide an ultimate explanation for the strengths of trophic interactions. The mechanistic basis of these rules has the potential to extend the predictive utility of theory beyond the environmental conditions and taxa in which trophic interaction strengths have been measured which has been a limitation to current statistical approaches to prediction[40]. Furthermore, the rules predict consistent saturation of predator feeding rates across prey densities, explain a slow-fast continuum in trophic interaction strengths, and predict the allometric scaling between predator and prey masses and functional response parameters.

Our rules suppose that functional responses emerge as the product of a long-term eco-co-evolutionary processes between predators, their prey, their own predators, and the environment [41–43]. A predator's fitness depends not only on its ability to procure food; it also depends on its ability to avoid its own predators, find mates, etc.[44]. Therefore, eco-evolutionary processes may combine such that trophic interaction strengths reflect the ability of a predator to minimally meet

its energetic demands during busts of low prey densities while also taking advantage of instances of booms at high prey densities. Many similarly complex behaviors and phenotypes of species are the product of many traits that are each under selection from a variety of forces. We believe that the approach we take here, focusing on the functional outcomes of these complex phenotypes, may be a useful way forward to understand and predict additional complex phenotypic outcomes and the ecological scaling relationships they produce.

The rules we derive also make specific, testable predictions regarding how the environment and global climate change are likely to influence trophic interaction strengths, as many of the parameters describing our rules are sensitive to the environment. For ectotherms, predator energetic demand is expected to increase with increasing temperature[2], whereas prey population size, body size and potentially energy density are likely to decrease[45–49]. These changes will alter the functional response parameters necessary to meet our rules and imply the potential for maladaptive trophic interaction strengths under climate change. Changes in parameters are also likely to occur over other environmental gradients, such as productivity gradients[50], which may allow for the prediction of changes in top-down interaction strengths and their consequences for ecosystems.

Given the success of our theory in predicting functional response parameters across field and laboratory studies, we believe this work will provide both useful predictions for empirical studies and the starting point for the development of additional theory. For example, our theory can predict which trophic interactions in communities are likely to be strong and, thus, have the potential to play outsized roles in structuring communities. Furthermore, current allometric food web models focus on modeling trophic systems in terms of the biomasses of species[11,18,19], whereas our work opens the potential to build allometric food web models based on individuals, a unit more closely aligned with evolutionary theory and ecological data. Third, although our theory has focused on pairwise trophic interactions, it provides the foundation for theory on generalist predators to embrace the additional complexity present in food webs in which predators consume multiple prey. Deepening our understanding of the ultimate causes governing trophic interaction strengths will assuredly provide important insights into the functioning and dynamics of ecosystems and their responses to ongoing global change.

Main References

1. Brown, J. H. *Macroecology*. (University of Chicago Press, 1995).
2. Brown, J. H., Gillooly, J. F., Allen, A. P., Savage, V. M. & West, G. B. Toward a Metabolic Theory of Ecology. *Ecology* **85**, 1771–1789 (2004).
3. Hatton, I. A., Dobson, A. P., Storch, D., Galbraith, E. D. & Loreau, M. Linking scaling laws across eukaryotes. *Proceedings of the National Academy of Sciences* **116**, 21616–21622 (2019).

4. De Ruiter, P. C., Neutel, A.-M. & Moore, J. C. Energetics, Patterns of Interaction Strengths, and Stability in Real Ecosystems. *Science* **269**, 1257–1260 (1995).
5. McCann, K., Hastings, A. & Huxel, G. R. Weak trophic interactions and the balance of nature. *Nature* **395**, 794–798 (1998).
6. Paine, R. T. Food-web analysis through field measurement of per capita interaction strength. *Nature* **355**, 73–75 (1992).
7. Yodzis, P. The stability of real ecosystems. *Nature* **289**, 674–676 (1981).
8. Coblentz, K. E., Novak, M. & DeLong, J. P. Predator feeding rates may often be unsaturated under typical prey densities. *Ecology Letters* **26**, 302–312 (2023).
9. Rall, B. C. *et al.* Universal temperature and body-mass scaling of feeding rates. *Phil. Trans. R. Soc. B* **367**, 2923–2934 (2012).
10. Uiterwaal, S. F. & DeLong, J. P. Functional responses are maximized at intermediate temperatures. *Ecology* **101**, e02975 (2020).
11. Yodzis, P. & Innes, S. Body Size and Consumer-Resource Dynamics. *The American Naturalist* **139**, 1151–1175 (1992).
12. Holling, C. S. The Components of Predation as Revealed by a Study of Small-Mammal Predation of the European Pine Sawfly1. *The Canadian Entomologist* **91**, 293–320 (1959).
13. Solomon, M. E. The Natural Control of Animal Populations. *Journal of Animal Ecology* **18**, 1–35 (1949).
14. Uiterwaal, S. F., Lagerstrom, I. T., Lyon, S. R. & DeLong, J. P. FoRAGE database: A compilation of functional responses for consumers and parasitoids. *Ecology* **103**, e3706 (2022).
15. DeLong, J. P. *Predator Ecology: Evolutionary Ecology of the Functional Response*. (Oxford University Press, Oxford, New York, 2021).
16. Pawar, S., Dell, A. I., & Van M. Savage. Dimensionality of consumer search space drives trophic interaction strengths. *Nature* **486**, 485–489 (2012).

17. Vucic-Pestic, O., Rall, B. C., Kalinkat, G. & Brose, U. Allometric functional response model: body masses constrain interaction strengths. *Journal of Animal Ecology* **79**, 249–256 (2010).

18. Brose, U., Williams, R. J. & Martinez, N. D. Allometric scaling enhances stability in complex food webs. *Ecology Letters* **9**, 1228–1236 (2006).

19. Otto, S. B., Rall, B. C. & Brose, U. Allometric degree distributions facilitate food-web stability. *Nature* **450**, 1226–1229 (2007).

20. Portalier, S. M. J., Fussmann, G. F., Loreau, M. & Cherif, M. Inferring Size-Based Functional Responses From the Physical Properties of the Medium. *Front. Ecol. Evol.* **9**, (2022).

21. Jeschke, J. M., Kopp, M. & Tollrian, R. Consumer-food systems: why type I functional responses are exclusive to filter feeders. *Biological Reviews* **79**, 337–349 (2004).

22. Okuyama, T. Prey density-dependent handling time in a predator-prey model. *Community Ecology* **11**, 91–96 (2010).

23. Armstrong, J. B. & Schindler, D. E. Excess digestive capacity in predators reflects a life of feast and famine. *Nature* **476**, 84–87 (2011).

24. McWilliams, S. R. & Karasov, W. H. Phenotypic flexibility in digestive system structure and function in migratory birds and its ecological significance. *Comparative Biochemistry and Physiology Part A: Molecular & Integrative Physiology* **128**, 577–591 (2001).

25. Secor, S. M., Stein, E. D. & Diamond, J. Rapid upregulation of snake intestine in response to feeding: a new model of intestinal adaptation. *American Journal of Physiology-Gastrointestinal and Liver Physiology* **266**, G695–G705 (1994).

26. Abrams, P. A. Functional Responses of Optimal Foragers. *The American Naturalist* **120**, 382–390 (1982).

27. Amarasekare, P. Ecological Constraints on the Evolution of Consumer Functional Responses. *Frontiers in Ecology and Evolution* **10**, (2022).

28. DeLong, J. P. & Coblentz, K. E. Prey diversity constrains the adaptive potential of predator foraging traits. *Oikos* **2022**, (2022).

29. Novak, M., Coblentz, K. E. & DeLong, J. P. In defense of the Type I functional response: The frequency and population-dynamic effects of feeding on multiple prey at a time. 2024.05.14.594210 Preprint at https://doi.org/10.1101/2024.05.14.594210 (2024).
30. Coblentz, K. E., Merhoff, S. & Novak, M. Quantifying the effects of intraspecific variation on predator feeding rates through nonlinear averaging. *Functional Ecology* **35**, 1560–1571 (2021).
31. Novak, M., Wolf, C., Coblentz, K. E. & Shepard, I. D. Quantifying predator dependence in the functional response of generalist predators. *Ecology Letters* **20**, 761–769 (2017).
32. Kleiber, M. Body size and metabolism. *Hilgardia* **6**, 315–353 (1932).
33. Damuth, J. Population density and body size in mammals. *Nature* **290**, 699–700 (1981).
34. Brown, J. H., Hall, C. A. S. & Sibly, R. M. Equal fitness paradigm explained by a trade-off between generation time and energy production rate. *Nat Ecol Evol* **2**, 262–268 (2018).
35. Brown, J. H., Mehlman, D. W. & Stevens, G. C. Spatial Variation in Abundance. *Ecology* **76**, 2028–2043 (1995).
36. Halley, J. & Inchausti, P. Lognormality in Ecological Time Series. *Oikos* **99**, 518–530 (2002).
37. Armstrong, R. A. & McGehee, R. Competitive Exclusion. *The American Naturalist* **115**, 151–170 (1980).
38. Grover, J. P. Resource Competition in a Variable Environment: Phytoplankton Growing According to Monod's Model. *The American Naturalist* **136**, 771–789 (1990).
39. Kiørboe, T. & Thomas, M. K. Heterotrophic eukaryotes show a slow-fast continuum, not a gleaner–exploiter trade-off. *Proceedings of the National Academy of Sciences* **117**, 24893–24899 (2020).
40. DiFiore, B. P. & Stier, A. C. Variation in body size drives spatial and temporal variation in lobster–urchin interaction strength. *Journal of Animal Ecology* **92**, 1075–1088 (2023).
41. Gutiérrez Al-Khudhairy, O. U. & Rossberg, A. G. Evolution of prudent predation in complex food webs. *Ecology Letters* **25**, 1055–1074 (2022).
42. Wickman, J., Litchman, E. & Klausmeier, C. A. Eco-evolutionary emergence of macroecological scaling in plankton communities. *Science* **383**, 777–782 (2024).

43. DeLong, J. P. Detecting the Signature of Body Mass Evolution in the Broad-Scale Architecture of Food Webs. *The American Naturalist* **196**, 443–453 (2020).
44. Jeschke, J. M. When carnivores are "full and lazy". *Oecologia* **152**, 357–364 (2007).
45. Amarasekare, P. & Savage, V. A Framework for Elucidating the Temperature Dependence of Fitness. *The American Naturalist* **179**, 178–191 (2012).
46. Atkinson, D. Temperature and Organism Size—A Biological Law for Ectotherms? in *Advances in Ecological Research* (eds. Begon, M. & Fitter, A. H.) vol. 25 1–58 (Academic Press, 1994).
47. Bernhardt, J. R., Sunday, J. M. & O'Connor, M. I. Metabolic Theory and the Temperature-Size Rule Explain the Temperature Dependence of Population Carrying Capacity. *The American Naturalist* **192**, 687–697 (2018).
48. Brett, J. R., Shelbourn, J. E. & Shoop, C. T. Growth Rate and Body Composition of Fingerling Sockeye Salmon, Oncorhynchus nerka, in relation to Temperature and Ration Size. *J. Fish. Res. Bd. Can.* **26**, 2363–2394 (1969).
49. Outhwaite, C. L., McCann, P. & Newbold, T. Agriculture and climate change are reshaping insect biodiversity worldwide. *Nature* **605**, 97–102 (2022).
50. Novak, M. Trophic omnivory across a productivity gradient: intraguild predation theory and the structure and strength of species interactions. *Proceedings of the Royal Society B: Biological Sciences* **280**, 20131415 (2013).

Methods

Databases, Data Handling, and Predictions

Our analyses relied on two data compilations: the FoRAGE compilation (Functional Responses Across the Globe in All Ecosystems) from[14], and the compilation of data on species mass, metabolic rates, and population densities from[3]. FoRAGE contains 3,013 functional response experiments, but we restricted our analyses to:

1) Studies including living prey that were not eggs. We did not include studies that used eggs as prey as it is unclear whether mass-abundance scaling relationships apply to eggs.
2) Studies with handling time estimates greater than $1x10^{-6}$. We did so following previous studies that have suggested that the studies within FoRAGE with lower values than the

cutoff are likely to include those for which the saturating Type II functional response had a poor fit to the data[8,10,39].

3) Studies that had both predator and prey masses. We excluded studies without this information because it is what allows a link between the FoRAGE database and empirical mass scaling relationships.

After excluding the studies that did not meet these criteria, we were left with 2162 functional response measurements.

We combined these two data compilations to obtain estimates of low and high prey densities likely to be experienced by predators (N_{low} and N_{high}), and predator energy demand (D). Specifically, we estimated N_{low} and N_{high} by using Bayesian log-log regressions of density in aerial m^2 on mass in g separately for prokaryotes, protists, ectotherm invertebrates, ectotherm vertebrates, mammals, and birds. Using the classification of prey and their masses in FoRAGE, we estimated the posterior predictive distribution for each of the interactions in FoRAGE and extracted the 10th and 90th percentiles as estimates of N_{low} and N_{high} respectively. To estimate D, we performed Bayesian log-log regressions of basal metabolic rate in kJ/d on predator mass in g separately for protists, ectotherm invertebrates, ectotherm vertebrates, mammals, and birds. We then used the median predicted metabolic rate of each predator in FoRAGE based on its classification and mass as our estimate of D. For each of the Bayesian regressions, we used flat priors on the intercept and slope, a Student t prior with degrees of freedom = 3, location = 0, and scale = 2.5. We approximated the posterior distribution using 1000 samples each from 4 Markov chains after a warmup of 1000 samples. We performed the Bayesian regressions using the R package 'brms'[51] using Stan[52] through the backend cmdstanr[53].

Combining the estimates of N_{low}, N_{high}, and D with the assumption that the degree of saturation of the predator functional response at the high prey density was 0.9 and the energy densities of prey were 5.6kJ/g [34], we then predicted the values of the space clearance rates and handling times for each predator-prey pair. We compared these predictions to observed values using reduced major axis regression through the R package 'lmodel2'[54].

Field-study Specific Predictions

Forty of the 2162 FoRAGE experiments were performed in the field. To avoid circularity, we excluded a subset of these because they estimated predator kill rates by using the proportion of predator diets consisting of a prey type coupled with the average mass of that prey and the predator's daily energetic demand to estimate the number of prey consumed per day. For the remaining studies, we performed a literature search to find information on predator energetic demand (D*)* and prey energy density (E). For energy demand, we used estimates of daily energy expenditure, if available. Otherwise, we used basal metabolic rate. For energy density, we used estimates of kJ/g if they were available. Otherwise, we used studies of prey body composition that gave the percent of prey body mass composed of protein and fat. We used conversions of 16.74 kJ/g for protein and 33.47 kJ/g of fat to calculate the total energy density of the prey in kJ/g [55,56]. We were able to find the requisite information for seven studies of six mammalian

predator-prey pairs. For these studies, we assumed the highest and lowest recorded prey densities as estimates of N_{low} and N_{high}. Details and references for the system-specific estimates are given in the Supplemental Information. As the estimate of mass, we used the mass in FoRAGE which was the mass reported in the study if possible[14].

Allometric Relationships

We derived equations for the space clearance rate and handling time assuming that predator energy demand (D) has a power law scaling with predator mass, that low and high prey densities (N_{low} and N_{high}) have power low scalings with prey mass, and that predator and prey masses have a power law scaling with one another. We assumed that the other variables determining space clearance rates and handling times are constants unrelated to predator or prey mass. Derivations of these equations are given in the Supplemental Information. We then used log-log regressions to test our predictions, obtaining estimates of the empirical relationships within FoRAGE across the different classifications used in the mass-abundance and mass-metabolism regressions between prey masses and abundances, predator masses and energy demand, and predator and prey masses (see *Databases and Data Handling*).

All analyses were performed in R using v. 4.3.1[57]

Methods References

51. Bürkner, P.-C. brms: An R Package for Bayesian Multilevel Models Using Stan. *Journal of Statistical Software* **80**, 1–28 (2017).
52. Stan Development Team. Stan Modeling Language Users Guide and Reference Manual, version 2.35. (2024).
53. Gabry, J., Češnovar, R., Johnson, A. & Bronder, S. *Cmdstanr: R Interface to 'CmdStan'*. (2024).
54. Legendre, P. *Lmodel2: Model II Regression*. (2018).
55. Chizzolini, R., Zanardi, E., Dorigoni, V. & Ghidini, S. Calorific value and cholesterol content of normal and low-fat meat and meat products. *Trends in Food Science & Technology* **10**, 119–128 (1999).
56. Menzies, A. K. *et al.* Activity, heart rate, and energy expenditure of a cold-climate mesocarnivore, the Canada lynx (Lynx canadensis). *Can. J. Zool.* **100**, 261–272 (2022).
57. R Core Team. *R: A Language and Environment for Statistical Computing*. (R Foundation for Statistical Computing, Vienna, Austria, 2023).

Acknowledgements

KEC and JPD were partially supported by a James S. McDonnel Foundation Studying Complex Systems Scholar grant and an NSF Organismal Responses to Climate Change (ORCC-2307464) grant to JPD. MN was supported by NSF DEB-2129758.

Author Contributions

KEC, MN, and JPD designed the research. KEC developed the theory with input from MN and JPD, performed the analyses, and wrote the first draft of the manuscript. All authors contributed to revisions.

Competing Interest Declaration

The authors declare no competing interests.

Data Availability Statement

Upon acceptance all of the data and code used in this manuscript will be made available as a permanently archived Github repository on Zenodo.